Civil Engineering and Architecture 11(3): 1372-1382, 2023 http://www.hrpub.org
DOI: 10.13189/cea.2023.110321

Correlations between Ground Motion Parameters Measures and Structural Damages of the Mw6.4, 2016 Meinong Taiwan Earthquake Using Hybrid Simulation Method

Boi Yee Liao[1,*], Sen Xie[2], Tsung-Shun Hsieh[3]

[1]Graduate Program of Engineering Technology Management, International College, Krirk University, Bangkok, Thailand
[2]International College, Krirk University, Thanon RamIntra, Khwaeng Anusawari, Khet Bang Khen, Krung Thep MahaNakhon 10220, Thailand
[3]Nanyang Institute of Management, 6 Eu Tong Sen Street #04-05, The Central 059817, Singapore

Received November 24, 2022; Revised January 6, 2023; Accepted January 28, 2023

Cite This Paper in the Following Citation Styles

(a): *[1] Boi Yee Liao, Sen Xie, Tsung-Shun Hsieh , "Correlations between Ground Motion Parameters Measures and Structural Damages of the Mw6.4, 2016 Meinong Taiwan Earthquake Using Hybrid Simulation Method," Civil Engineering and Architecture, Vol. 11, No. 3, pp. 1372 - 1382, 2023. DOI: 10.13189/cea.2023.110321.*

(b): *Boi Yee Liao, Sen Xie, Tsung-Shun Hsieh (2023). Correlations between Ground Motion Parameters Measures and Structural Damages of the Mw6.4, 2016 Meinong Taiwan Earthquake Using Hybrid Simulation Method. Civil Engineering and Architecture, 11(3), 1372 - 1382. DOI: 10.13189/cea.2023.110321.*

Abstract The purposes of this research are to invest the correlations of ground motion parameters, including characteristic intensity (Ic), standardized version of cumulative absolute velocity (CAVstd), maximum incremental velocity (MIV), and the relationships with the damages of the buildings caused by the Mw6.4, 2016 Meinong Taiwan earthquake. To detect the validations of the hybrid simulation method, the waveforms of three stations near the epicenter are simulated and compared with the observations by employing the inverted source model of the Meinong earthquake. The comparisons between the observations and simulations demonstrate that the PGAs of the observations and simulations are well consistent and underestimations of the high-period contents are improved. Based on the excellent results of the method, the three parameters around Tainan city are calculated and displayed in this research. Apparently, most of the higher values of the three parameters distribute around the north-western regions of the epicenter of the Meinong earthquake, which coincides with the rupture direction of the earthquake toward the northwest. Almost all of the damaged buildings are located well within the values of MIV with 30cm/s, Ic with 316cm1.5/s2.5, and CAVstd with 418cm/s, indicating both of the results are agreeable to the previous studies and offering critical values of the three parameters to predict the potential earthquake-induced damages of buildings. Finally, we discover that two in pairs of the three parameters have high correlation coefficients and exceptional linear relationships between them. The correlation coefficient between MIV and Ic is 0.88, between MIV and CAVstd is 0.89, and between CAVstd and Ic is 0.99. The linear regression models of a couple of parameters are established to model linear predictor functions.

Keywords Maximum Incremental Velocity, Characteristic Intensity, Standardized Version of Cumulative Absolute Velocity, Hybrid Simulation Method

1. Introduction

Extracting some parameters from seismic recordings to correlate damages to buildings and structural design is important to work for earthquake engineering when an earthquake with a large magnitude occurs. In the past

decades, many parameters from ground motions had been offered to describe the damage potential of an earthquake. For example, the strong motion recorded signals in terms of peak (PGA, PGV, and PGD) were applied well to seismic risk assessments [1]. Many parameters contain energy response, strong motion duration, and frequency contents of strong motion also strongly affected the damage potential of ground motions [2, 3]. Liao, et al. [4] employed a seismic spectral intensities system (SIs) to evaluate the damages of buildings with different heights for a potential earthquake in central Taiwan. Based on the excellent effects of SIs, a good correlation between the damages to the buildings caused by the 2016 Meinong earthquake and SIs was observed in [5]. Considering the energy with the significant duration of a strong motion, Danciu and Tselentis [6] thought that the characteristic intensity was an outstanding index that can correlate the structural damages of buildings due to maximum deformation energy with the destructiveness of an earthquake well. The regression relation between Ic and the maximum displacement at the roof was offered in [7] to predict the responses of buildings affected by an earthquake using near and far fault recordings. Massumi and Gholami [8] indicated the effect of IC on inter-story drift and roof was evident and correlated with the structural period. As the structural period decreases, the effect will increase. Cumulative absolute velocity contains factors including waveform, amplitude, and duration time of a seismic recording; therefore, it is believed that CAV is a more reliable parameter to measure the destructiveness of an earthquake than just using PGA. Cabanas, et al. [9] regressed the CAV with observed damage in type A structure well and suggested that CAV can be a criterion to estimate the damage by ground motion. Employing the PEER-NGA database to develop GMPEs (Ground-Motion Prediction Equations) for CAV, Campbell, and Bozorgnia [10] claimed that CAV was a powerful parameter to rapidly evaluate the potential damages to structures after an earthquake occurs. Wu et al. [11] developed a GMPE of CAV for seismic hazard assessment in Taiwan and demonstrate their results can correspond to the occurrence probability of earthquakes in 50 years of Taipei, Taiwan. Additionally, the maximum incremental velocity is acknowledged as one of the most important factors affecting the inelastic displacement ratios of a structure [12]. Zhai, et al. [13] detected the influences of MIV on inelastic displacement ratio spectra (IDRS) and discovered that the impacts of MIV are inversely proportional to the period ranges of structures. The MIV is considered an important parameter to be applied to the aseismic design of buildings and structures. On the basis of the PEER-NGA (2009), ground motion database, Guaman, et al. [14] derived the empirical attenuation law of MIV with magnitude and site parameters and offered the relationship between MIV and PGA. The 2016 Meinong earthquake struck southern Taiwan, inflicting 117 casualties and 551 injuries [15]. Establishing the intensity parameters thresholds corresponding to damages and mitigating the earthquake disasters in the future are significant works, especially in earthquake-prone areas. In this study, firstly the hybrid simulation method which combines the low-frequency components (f ≦ 1Hz) by theoretical simulation and high-frequency components (1Hz<f ≦ 20Hz) by the semi-empirical technique are used to simulate the recordings around Tainan city according to the source model of 2016 Meinong earthquake [5]. Secondly, the three parameters Ic, CAVstd, and MIV are calculated by the simulated recordings to correlate with the observed damages in the 2016 Meinong earthquake and compared with the previous studies. Finally, we discuss the relationships between the parameters for disaster prevention.

2. Methodology

2.1. Hybrid Simulation

The representation theorem describes the displacement recording Uk(x,t) at position x and time t is expressed [16]

$$U_k(x,t) = \int_{\Sigma} m_{pq}(\xi,t) * \frac{\partial G_{kp}(x,\xi,t-t^r(\xi))}{\partial \xi_q} d\Sigma \quad (1)$$

where Σ is a subevent of the rupturing fault, mpq is the seismic moment density tensor, ξ is the position on the subfault, Gkp is the Green's function tensor, tr is rupture time, and $*$ represents convolution operation. If only considering the effects of shear stress on the fault, eq.(1) can be modified as

$$U_k(x,t) = \int_{\Sigma} \mu \Delta u(\xi) s\big(\xi, t - t^r(\xi)\big)(n_p \nu_q + n_q \nu_p) * \frac{\partial G_{kp}(x,\xi,t)}{\partial \xi_q} d\Sigma \quad (2)$$

where μ means shear modulus, $\Delta u(\xi)$ is the final slip, $s(\xi,t)$ represents slip function, n and ν are the vectors on the fault plane. If the fault plane is divided into nL*nW subfaults, the seismic wave to an observation station which locates at position x is the summation from all the subfaults. Eq. (2) can be discretized as following

$$U_k(x,t) = \sum_{i=1}^{n_L} \sum_{j=0}^{n_W} \mu \Delta u_{ij} s_{ij}\big(t - t_{ij}^r\big)(n_p \nu_q + n_q \nu_p) * \frac{\partial G_{kp}(x,\xi,t)}{\partial \xi_q}\Big|_{\xi=\xi_{ij}} \Delta\Sigma \quad (3)$$

The hybrid method of Pulido and Kubo [17] is employed for modeling broadband seismic waves. Essentially, the low-frequency portions (f≦1Hz) of a seismic wave are deterministic, but the high-frequency portions (1Hz<f≦20Hz) are affected by the heterogeneity of the source model so they tend to be stochastic processes. To fulfill the simulation of the low-frequency portions, the method of Hisada [18] is used to calculate eq. (3). The semi-empirical stochastic method described in [19] is applied to complete the high-frequency portions. Finally, the seismic recording Uk(x,t) can be obtained by combining the two portions of different frequency bands together.

2.2. Intensity Parameters

Based on the previous studies, three intensity parameters Ic, CAVstd and MIV are highly correlated with the structural damage of buildings by an earthquake of large magnitude. The characteristic intensity (Ic) is expressed as

$$I_c = a_{rms}^{1.5} t_s^{0.5} \quad (4)$$

$$a_{rms} = \sqrt{\frac{1}{t_r}\int_0^{t_r}[a(t)]^2 dt} \quad (5)$$

where a(t) is an acceleration time history, tr means the total duration of the ground motion, and ts represents significant duration time which is the interval between the times at which5% and 95% of the Arias intensity [6].

The standardized version of cumulative absolute velocity (CAVstd) means filtering out some low-amplitude, non-damaging ground motions (under 0.025g) to be a potential intensity measure related to damages. It is defined as [10]

$$CAV_{std} = \sum_{i=1}^{N}(H(PGA_i - 0.025)\int_{i-1}^{i}|a(t)|dt) \quad (6)$$

where N is the number of non-overlapping one-second time intervals, PGA is the peak ground acceleration (g) in time interval i, and H(x) is the Heaviside step function.

The maximum incremental velocity (MIV) is defined as the maximum area under the acceleration time history between two successive zero-crossings. It is expressed as

$$MIV = \max(\int_{t_i}^{t_{i+1}}|a(t)|dt) \quad (7)$$

In near-fault regions, the source directivity effect may produce a long-duration pulse of fling which can destroy these buildings seriously. From Eq.(7), MIV which considers both amplitude and duration time of a(t) is an appropriate parameter to measure potential structural damage.

3. Theoretical Test

3.1. Comparisons between Synthetic and Observed Recordings of Meinong Earthquake

To identify the validity of the hybrid method, we synthesize strong motions at three stations CHY061, CHY063 and CHY065 around the epicenter of the Meinong earthquake and compare them with the observed strong motions. The locations of three stations are shown in Figure 1. Based on the inverted source model of the Meinong earthquake [5] in Figure 2 and the layered model (table 1 [20]), the entire synthetic waveforms are calculated by the hybrid method. The synthetic results with observed recordings (EW component) are demonstrated in Figure 3.

From Figure 3, there are three important results that are definitely worth discussing. At first, the differences of PGAs between observed and synthetic waveforms are less than 9% of relative errors. It reveals that the PGAs of recordings may be strongly dominated by the source effect of the earthquake because the three stations are close to the epicenter of the earthquake. Secondly, we transformed the simulated and real recordings into pseudo-absolute acceleration (Sa) with damping of 0.05. The synthetic Sa almost agree with the real one and the high-period (low-frequency) contents are improved obviously. The underestimation of low-frequency contents is a traditional problem due to the limitation of stochastic simulation. To overcome this flaw, we calculate the low-frequency contents (f≦1Hz) theoretically to get suitable estimations. In addition, the high-frequency contents of simulated waveforms are in the accordance with real ones in Sa, indicating the semi-empirical method can suppress the overestimation of high-frequency contents by using correction function offered by Irikura et al. [21]. Finally, almost the main energies and duration times of synthetic waveforms are consistent with the real waveforms. It means that the hybrid method can capture main characteristics of real recordings well. However, if the local site effect at the station could be understood in advance, the differences between PGA and duration time may be reduced. The detailed site effect could play an important role in simulating an entire seismic waveform. In spite of the simulated waveforms are not consistent with the real ones perfectly, the parameters Ic, CAVstd and MIV are associated with the energy-based intensity measures of a(t) and can be perceived as an averaged effect related a(t) from Eq. (5)~(7), therefore, the errors between the simulated and real waveforms don't affect largely the estimations of the three parameters.

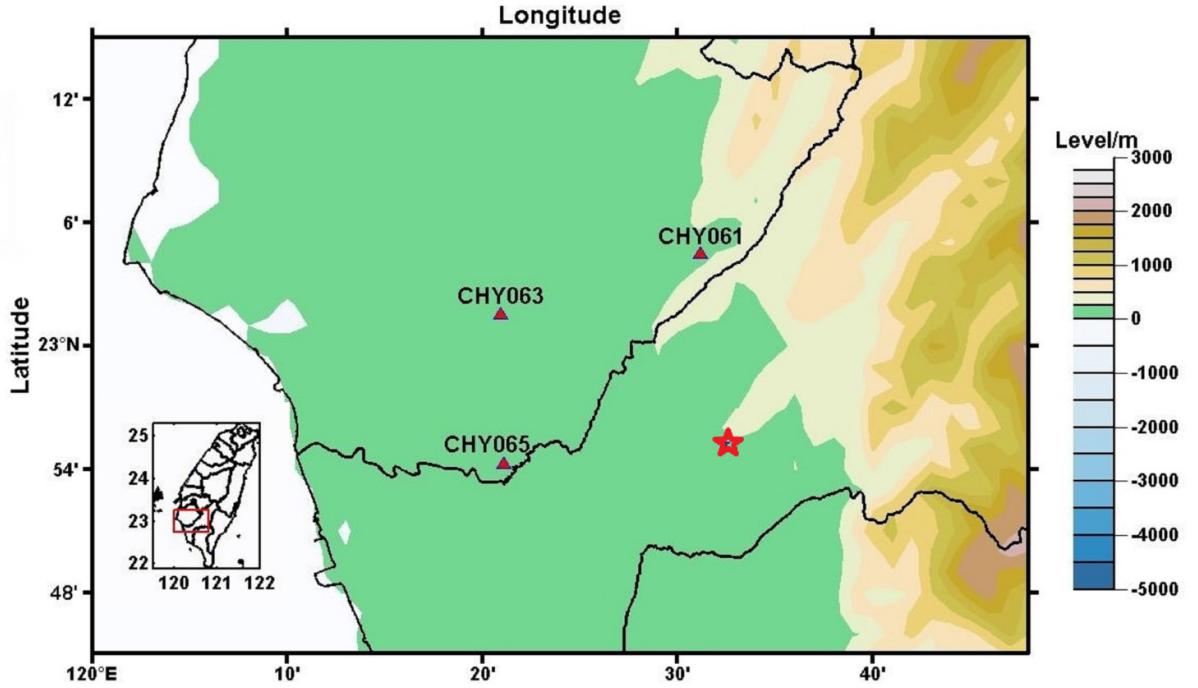

Figure 1. The locations of three stations CHY061, CHY063 and CHY065 are represented as red triangles. The epicenter of Meinong earthquake is represented as red star

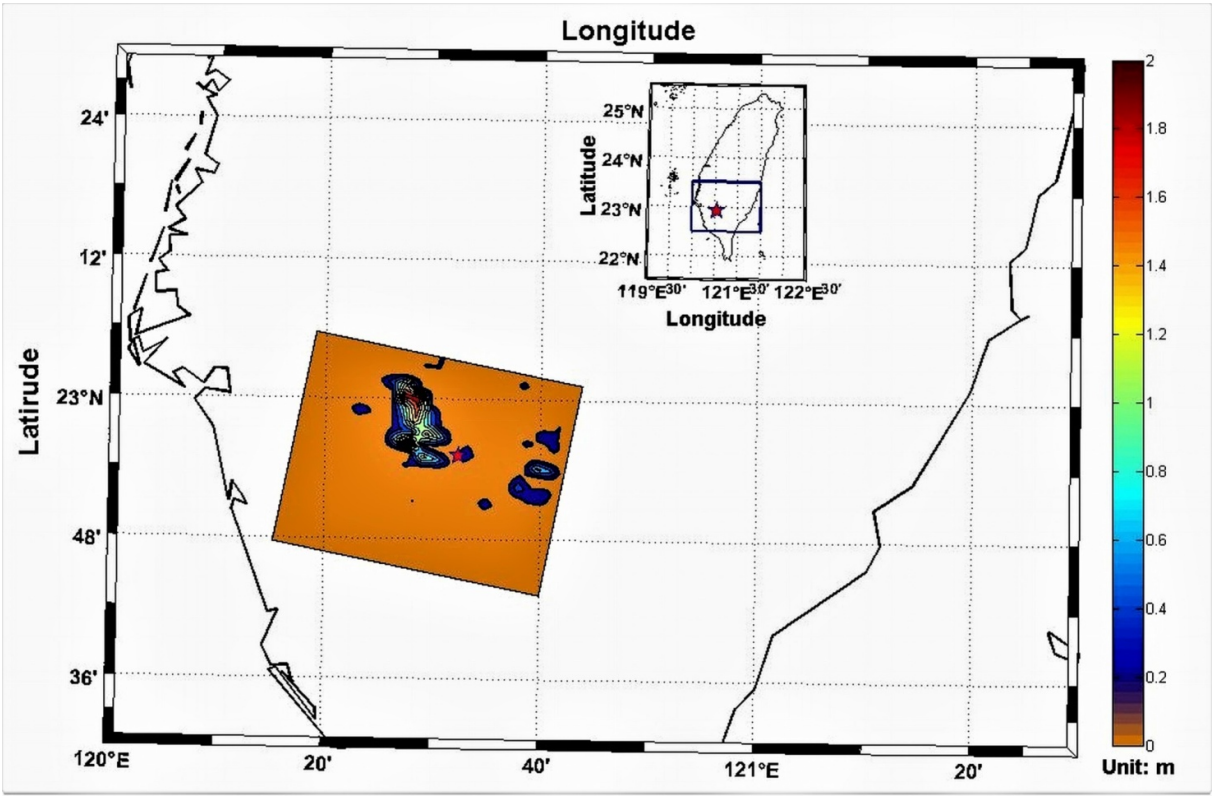

Figure 2. The inverted source model of Meinong earthquake (Mw 6.4) by using the hybrid homomorphic deconvolution is cited from [5]

Table 1. The layer crustal structure used in the waveform simulation [20]

Layer	H (km)	Vp (km/s)	Vs(km/s)	ρ (g/cm3)	Qp	Qs
1	0.5	3.50	1.99	2.4	600	300
2	2.5	4.41	2.65	2.4	600	300
3	3.0	5.01	3.03	2.5	600	300
4	4.0	5.43	3.22	2.6	600	300
5	5.0	5.77	3.29	2.6	600	300
6	5.0	5.82	3.30	2.6	600	300
7	5.0	5.99	3.41	2.6	600	300
8	5.0	6.44	3.63	2.6	600	300
9	5.0	6.96	3.94	2.6	600	300
10	5.0	7.54	4.25	2.7	600	300
11	5.0	7.74	4.50	2.7	600	300
12	5.0	7.97	4.53	2.7	600	300
13	5.0	8.24	4.54	2.7	600	300

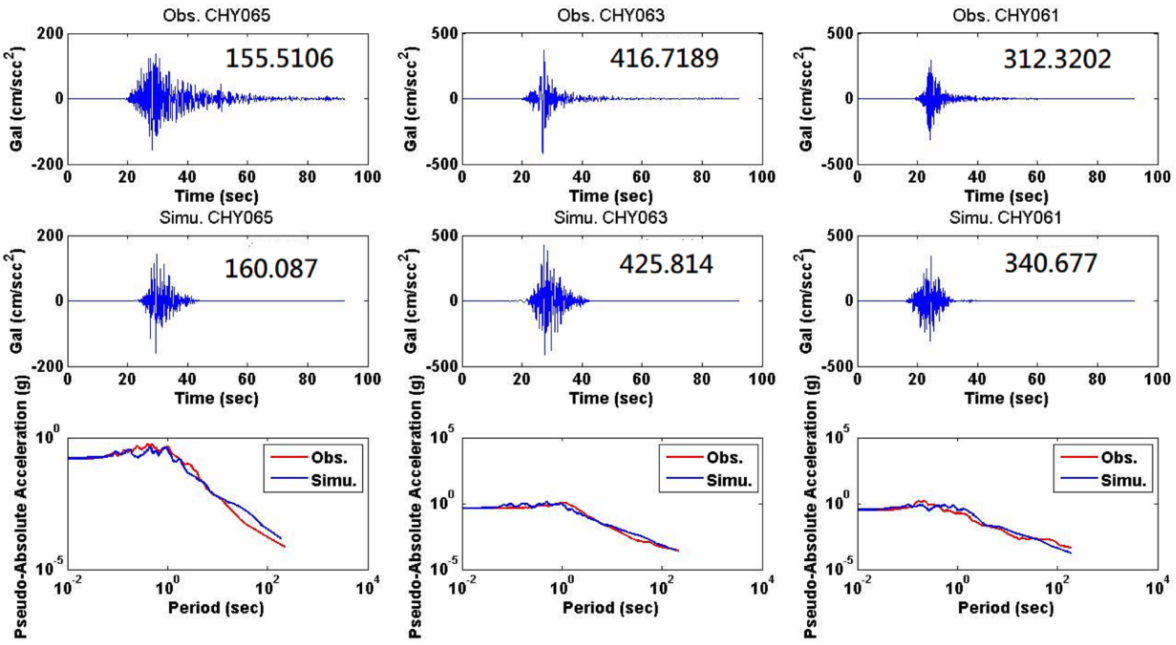

Figure 3. The comparisons between observed and simulated waveforms are shown. The first row demonstrates the observed waveforms at three stations CHY065, CHY063 and CHY061. The numbers beyond the waveforms represent the PGAs of the three recordings. The second row demonstrates the simulated waveforms of the three stations and the numbers beyond the waveforms represent the simulated PGAs. The third row demonstrates the pseudo-absolute accelerations (Sa) of the observed and simulated waveforms. The red line is the observed Sa and the blue line is the simulated one. It is apparent that the difference between observed and simulated PGA is less than 8% of relative error and the simulated Sa is quite consistent with the Sa of the observed waveform

4. Results and Discussions

Combining the source model of the Meinong earthquake with the hybrid method, we calculate the three parameters around Tainan city. Figures 4, 5 and 6 display the distributions of CAVstd, Ic and MIV, respectively. Most of the higher values of the three parameters locate around the north-western direction of the epicenter, coinciding with the rupture direction of the source effect [22]. It reveals that the source effect strongly affects the three parameters close to the epicenter of the Meinong earthquake, and conversely, the three near-field parameters can also reflect some information about the source effect. All the damaged buildings are represented as white squares located within the contour with 481cm/s of CAVstd. According to the research results in [23], the catastrophic threshold value of CAVstd is about 481cm/s, which is agreeable to our finding. As shown in Figure 5, there are 94% of damaged buildings locating within the contour with 316cm/s of Ic. It is coincident that the damage threshold of Ic can correspond to 316cm/s approximately, based on the relationship between the maximum global drift ratio (MGDR) and Ic [7]. In addition, the IDRS of buildings with a period range between 0.2s-1.5s are significantly affected by the near-field ground motions and MIV has a larger effect than PGV on IDRS [13]. Coincidently, on a basis of the investigations of the disaster area, most of the buildings damaged by the Meinong earthquake had a corresponding period range from 0.1s to 1.6s. Therefore, MIV could be a suitable indicator to evaluate potential damage. In Figure 6, all the damaged buildings sit within the contour with 30cm/s of MIV, which indicates 30cm/s is exactly a threshold of MIV and has reference value to disaster management. In the following, the three parameters are used to detect the relationships between them considering near-field simulations. Figures 7, 8 and 9 demonstrate the regression relationships of Ic with MIV, CAVstd with MIV and Ic with CAVstd, respectively. It is worth noting that the relationship between both parameters seems linear. The Ic is the most correlated to the CAVstd and can predict CAVstd with the highest efficiency. In Figure 7, some parts of the differences between Ic and the regression line tend to increase with Ic. From the definition of Ic and MIV, we speculate that the increase of arms may correspond to the increase of ts and some values of Ic may change dramatically. But the MIV of a(t) wouldn't make large variations with the increasing duration time tr, therefore, the phenomenon appears in Figure 7. The regression relationship between CAVstd with MIV shown in Figure 8 is better than the relationship of Ic with MIV. Based on Eq. (6) and (7), the MIV and CAVstd are highly related and the better relationship between MIV and CAVstd is in accordance with expectations normally. Figure 9 shows the perfectly linear regression relationship between Ic and CAVstd. It is trivial that both of the two parameters are energy-based from Eq. (4) and (6). Ic and CAVstd are just different types of applications about the energy of a(t). The linear relationship between Ic and CAVstd is necessary and inevitable, which is modeled as

$$CAVstd=1.4146*Ic+40.1832 \quad (8)$$

The correlation coefficient between them reaches to 0.99. Based on the presented results, we demonstrate that establishing a quantified relation between strong ground motion and earthquake damage can be implemented by using suitable parameter. In this research, the Ic, CAVstd and MIV are employed to correlate the damage to buildings caused by the 2016 Meinong earthquake. Comparing the locations of damage with the parameters, the thresholds of the three parameters for the damage are well founded and valuable for disaster prevention. However, the value of the threshold may depend on the magnitude and source model of the earthquake, geologic configurations near the buildings and the styles of buildings. In further study, statistical analyses will be applied to the resulting data from the previous earthquake disasters to extract a statistical model for estimating post seismic damage status of structures based on seismic parameters.

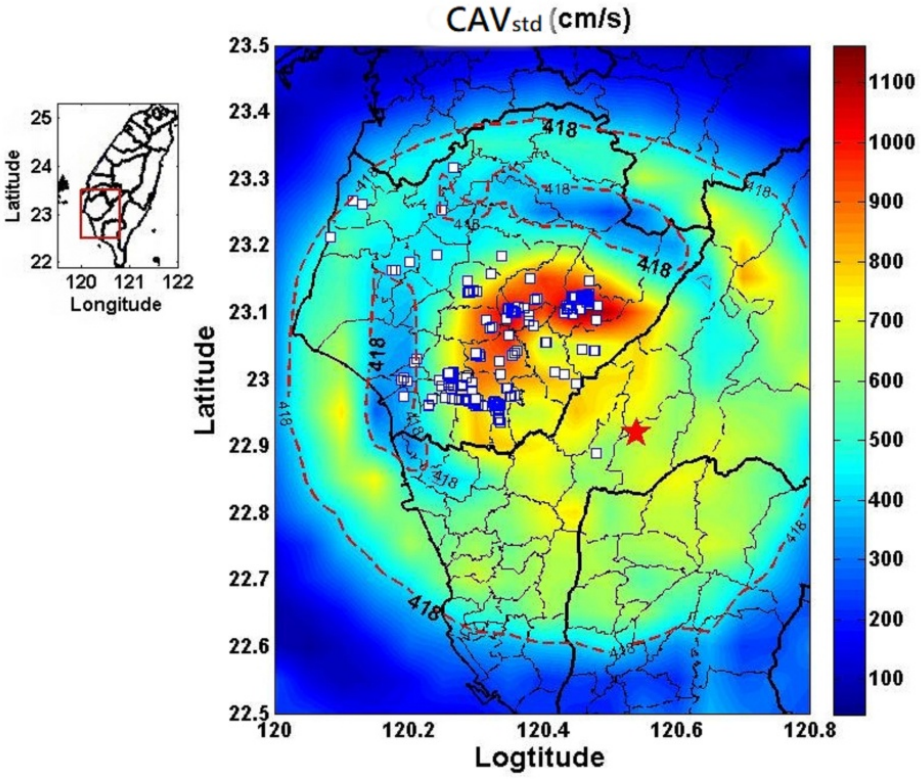

Figure 4. The distribution of the standardized version of cumulative absolute velocity (CAVstd) caused by the Meinong earthquake Mw 6.4. The red star is the epicenter of Meinong earthquake and the white squares represent as damaged building. The higher values of CAVstd accumulated at the west-northern parts of the epicenter. All the damaged buildings are at the places with CAVstd larger than 418cm/s.

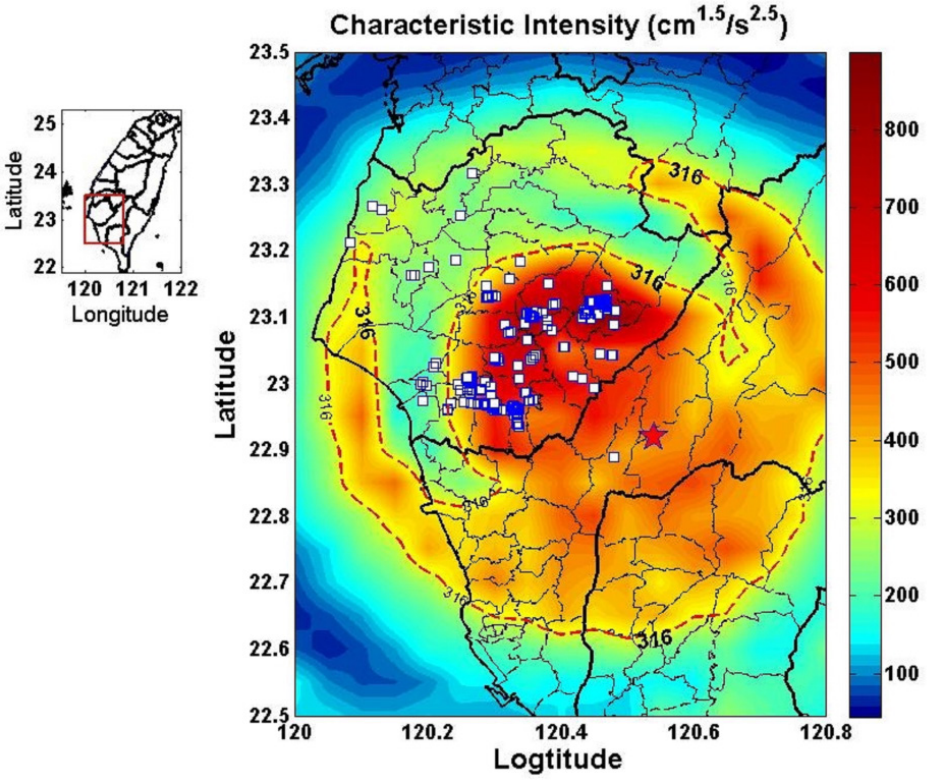

Figure 5. The distribution of the characteristic intensity (Ic) caused by the Meinong earthquake Mw 6.4. The red star is the epicenter of Meinong earthquake and the white squares represent as damaged building. The higher values of Ic accumulated at the west-northern parts of the epicenter. Most of the damaged buildings are at the places with Ic larger than 316cm1.5/s2.5.

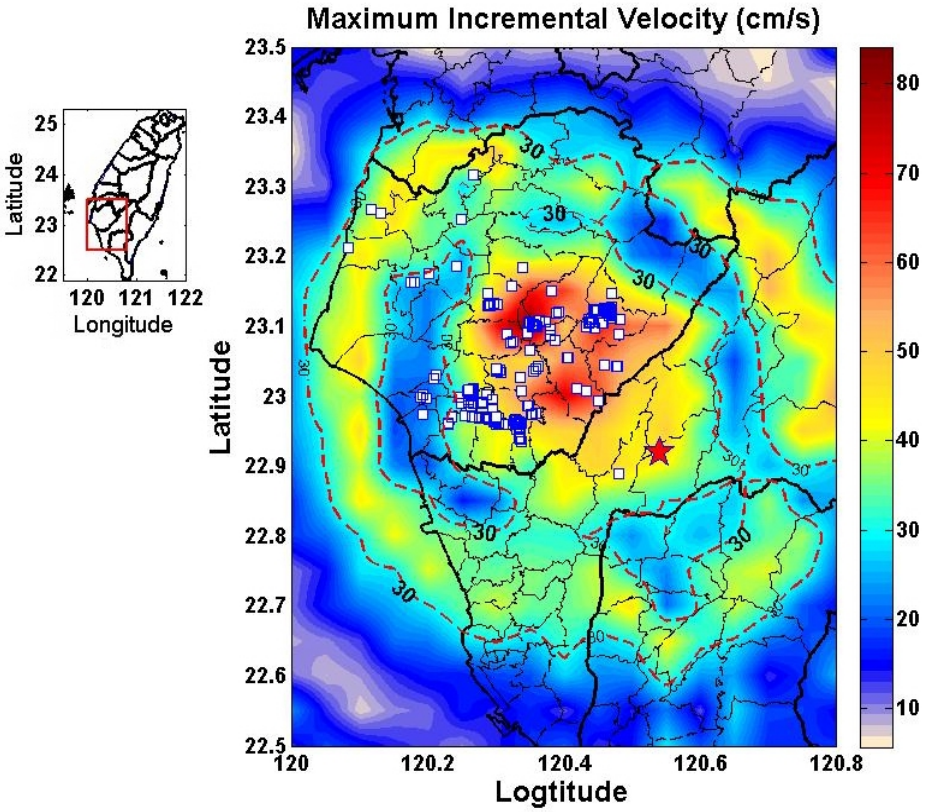

Figure 6. The distribution of the maximum incremental velocity (MIV) caused by the Meinong earthquake Mw 6.4. The red star is the epicenter of Meinong earthquake and the white squares represent as damaged building. The higher values of MIV accumulated at the west-northern parts of the epicenter. All the damaged buildings are at the places with MIV larger than 30cm/s.

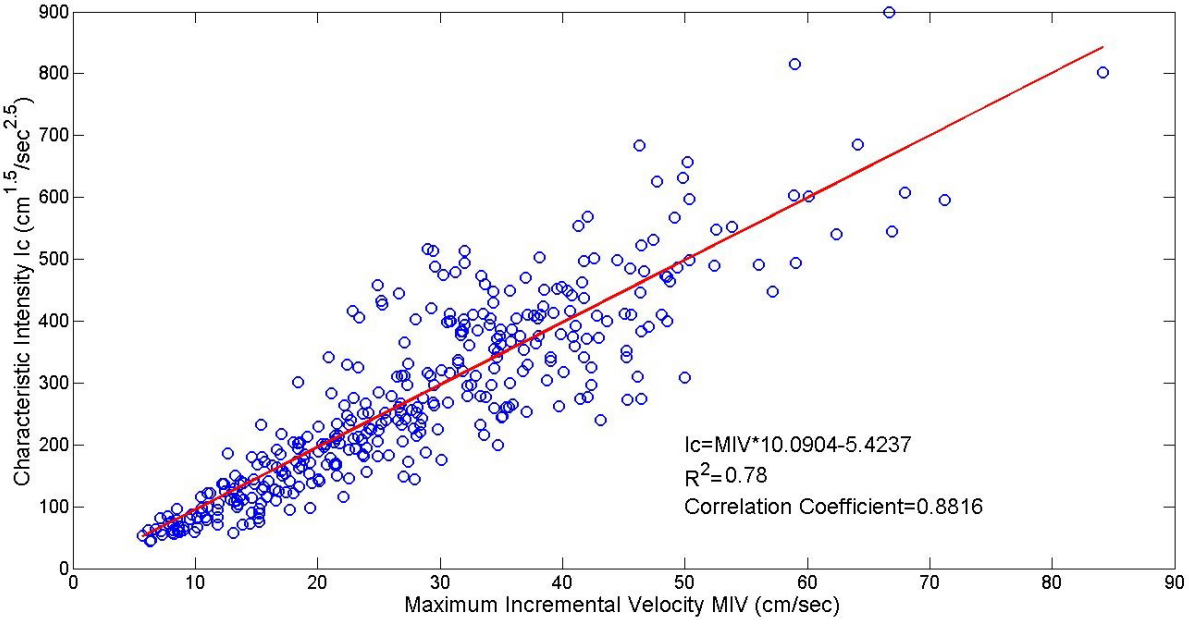

Figure 7. The regression relationship between MIV and Ic is shown as Ic=MIV*10.0904-5.4237

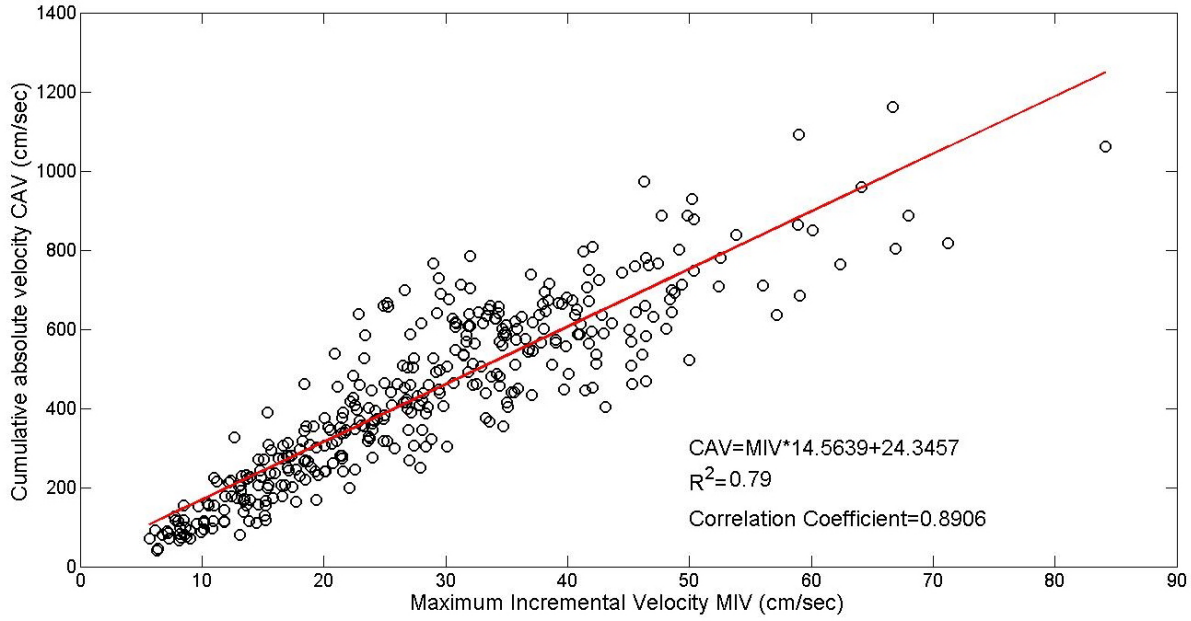

Figure 8. The regression relationship between MIV and CAVstd is shown as CAVstd=MIV*14.5639+24.3457

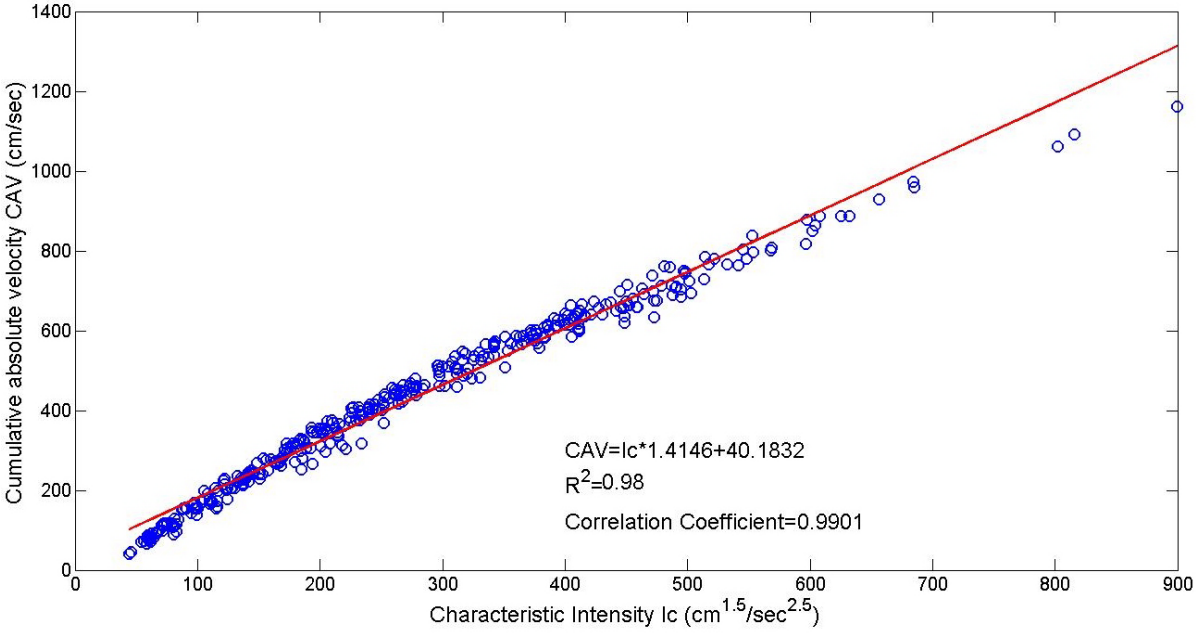

Figure 9. The regression relationship between Ic and CAVstd is shown as CAVstd=Ic*1.4146+40.1832

5. Conclusions

The investigation of interdependency between the seismic parameters and damage to buildings caused by large earthquakes is crucial work in risk assessment. One of the efficient methods is employing a large number of observed recordings to establish a statistical model for predicting the strong motions and parameters [24, 25]. However, the error values between the estimated and observed tend to be great for the regions with small data. By contrast, the physical-based numerical simulation is gradually playing a promising role in reflecting the characteristics of the ground motions with the source rupture, the propagation path and complex site effects in shallow geology [26]. In summary, the contributions of this study demonstrate that the physical-based hybrid simulation method can be applied: 1.) to complement near-source recordings, especially in those regions where the data are spare, for estimating the earthquake ground motion parameters Ic, CAVstd and MIV which are

calculated based on waveforms, 2.) to obtain the correlations between the earthquake ground motion parameters and source effect, 3.) to detect the relationships between the damages caused by earthquake and the thresholds of the three earthquake ground motion parameters Ic, CAVstd and MIV, 4.) to provide waveforms for scenarios of region-specific hazard and risk assessments for protecting the safety of the people and reducing the loss in functionality of facilities, roads, pipelines, and other lifelines from the earthquake disaster, 5.) to regress the relationships between couples of parameters.

In this research, the hybrid simulation method and source model of the Meinong earthquake are used to calculate three parameters CAVstd, Ic, and MIV around Tainan city for measuring the damages to buildings caused by the 2016 Meinong earthquake (Mw 6.4) Taiwan. The hybrid method can improve the underestimate of low-frequency and suppress the high-frequency contents to contribute to better waveform simulation. The positions with higher values of the three parameters are coincident with the source rupture direction, revealing the source rupture directivity strongly affects the values of the three parameters in near-source regions. The three parameters CAVstd, Ic, and MIV are correlated with maximum deformation energy, damages of structures and inelastic displacement ratio spectra, respectively, so the three parameters are excellent indexes to estimate the structural damages due to strong earthquakes. Most of the damages to the buildings are almost located in the areas with CAVstd>418cm/s, Ic>316cm1.5/s2.5 and MIV>30cm/s. The thresholds of the three parameters (CAVstd, Ic, MIV) may be represented as (418cm/s, 316cm1.5/s2.5, 30cm/s) for disaster relief supplies, and disaster prevention information management. The linear relationships between both parameters are very obvious, especially the Ic-CAVstd regression relationship.

Acknowledgement

The authors would like to express their thanks to two anonymous reviewers for their valuable suggestions and to the financial support by the Krirk University.

REFERENCES

[1] Masi A., ·Chiauzzi L., Braga F., Mucciarelli M., Vona M., Ditommaso R., "Peak and integral seismic parameters of L'Aquila 2009 ground motions: observed versus code provision values", Bulletin of Earthquake Engineering, vol 9, pp. 139-156, 2011. DOI: 10.1007/s10518-010-9227-1.

[2] Alvanitopoulos, P.F., Andreadis, I., Elenas, A., "Interdependence between damageindices and ground motion parameters based on Hilbert–Huang transform", Meas. Sci. Technol. vol.21 (2), pp. 025101, 2010. DOI: 10.1088/0957-0233/21/2/025101.

[3] Elenas, A., "Intensity parameters as damage potential descriptors of earthquakes. In:Computational Methods in Stochastic Dynamics". Springer, Dordrecht, pp. 327–334. 2013.

[4] Liao, B. Y., Liu, C. H., Sheu T, W., Yeh, Y. T., "Earthquake hazard in central Taiwan evaluatedusing the potentially successive 2013 Nantou Taiwan earthquake sequences", Geomatics, Natural Hazards and Risk, vol. 11, pp. 678-697, 2020. DOI: https://doi.org/10.1080/19475705.2020.1745901

[5] Liao, B. Y., Huang, H. C. Xie, S., "The Source Characteristics of the Mw6.4, 2016 Meinong Taiwan Earthquake from Teleseismic Data Using the Hybrid Homomorphic Deconvolution Method", Applied Sciences, vol. 12, pp. 494, 2022. DOI: https://doi.org/10.3390/app12010494

[6] Danciu, L., Tselentis, G. A., "Engineering Ground-Motion Parameters Attenuation Relationships for Greece", Bulletin of the Seismological Society of America, Vol. 97, pp. 162–183, 2007. DOI: 10.1785/0120040087

[7] Vargas-Alzate, Y.F., Hurtado, J.E., "Efficiency of Intensity Measures Considering Near- and Far-Fault Ground Motion Records", Geosciences, vol. 11, pp. 234, 2021. DOI: https://doi.org/10.3390/geosciences1106023

[8] Massumi, A., Gholami, F., "The influence of seismic intensity parameters on structural damage of RC buildings using principal components analysis", Applied Mathematical Modelling, vol. 40, pp. 2161-2176, 2016. https://doi.org/10.1016/j.apm.2015.09.043.

[9] Cabanas, L., Bemito, B., Herraiz, M., "An approach to the measurement of the potential structural damage of earthquake ground motions", Earthquake engineering & structural dynamics, vol. 26, pp. 79-92, 1997. https://doi.org/10.1002/(SICI)1096-9845(199701)26:1%3C79::AID-EQE624%3E3.0.CO;2-Y

[10] Campbell, K.W., Bozorgnia, Y., "A ground motion prediction equation for the horizontal component of cumulative absolute velocity (CAV) using the PEER-NGA database", Earthquake Spectra, vol. 26, pp. 635–650, 2010. https://doi.org/10.1193/1.4000012.

[11] Xu, Y., Wang, J. P., Wu, Y. M., Kuo-Chen, H., "Prediction models and seismic hazard assessment: A case study from Taiwan, Soil Dynamics and Earthquake Engineering", vol.122, pp. 94-106, 2019.https://doi.org/10.1016/j.soildyn.2019.03.038.

[12] Baez, J. I., Miranda, E., "Amplification Factors to Estimate Inelastic Displacement Demands for the Design of Structures in the Near Field", Proceedings of the 12th Word Conference on Earthquake Engineering, Auckland, New Zealand: New Zealand Society for Earthquake Engineering, pp. 1561, 2000.

[13] Zhai, C., Li, S., Xie, L., "Study on inelastic displacement ratio spectra for near-fault pulse-type ground motions", Earthq. Eng. Eng. Vib. vol. 6, pp. 351–355, 2007. https://doi.org/10.1007/s11803-007-0755-x

[14] Guaman, J., Kirkner, D., Kurama, Y., "Empirical Ground

Motion Attenuation Relationships for Maximum Incremental Velocity", Proceedings of the 9th U.S. National & 10th Canadian Conference on Earthquake Engineering, Toronto, CA. 2010.

[15] Lin, Y.Y., Yeh, T.Y., Ma, K.F., Song, A.T.R., Lee, S.J., Huang, B.S., Wu, Y.M., "Source characteristics of the 2016 Meinong (ML 6.6), Taiwan, earthquake, revealed from dense seismic arrays: Double sources and pulse-like velocity ground motion", Bulletin of the seismological society of America, vol. 108, pp. 188–199, 2018. https://doi.org/10.1785/0120170169.

[16] Aki, K., Richard, P. G., "Quantitative Seismology", W. H. Freemen and Company, San Franscico., 1980.

[17] Pulido, N., Kubo, T., "Near-fault strong motion complexity of the 2000 Tottori earthquake (Japan) from a broadband source asperity model", Tectonophysics, vol. 390, pp. 177-192, 2004.

[18] Hisada, H., "An efficient method for computing Green's functions for a layered half-space with sources and receivers at close depths (part 2)", Bull. Seism. Soc. Am. vol. 85, pp. 1080-1093, 1995.

[19] Liao, B. Y., Xie, S., "Landslide Hazard Assessments of A Potential Earthquake-triggered in Central Taiwan Using Newmark's Model with the Stochastic Semi-Empirical Technique", Civil Engineering and Architecture, vol. 10, pp. 2877-2885, 2022. DOI: 10.13189/cea.2022.100708.

[20] Lin, Y. Y., Yeh, T. Y., Ma, K. F., Alex Song, T. R., Lee, S. J., Huang, B. S., Wu, Y. M., "Source Characteristics of the 2016 Meinong (ML 6.6), Taiwan, Earthquake, Revealed from Dense Seismic Arrays: Double Sources and Pulse-like Velocity Ground Motion", Bull. Seism. Soc. Am. vol. 108, pp. 118-199, 2018.

[21] Irikura K., Kagawa T., Sekiguchi H., "Revision of theempirical Green's function method by Irikura 1986," Programme and abstracts. Seismol Soc Jpn, vol. 2, pp. B25, 1997.

[22] Yang, Y.H., Chen, Q., Diao, X., Zhao, J.J., Xu, L., Hu, J.C., "New interpretation of the rupture process of the 2016 Taiwan MeinongMw 6.4 earthquake based on the InSAR, 1-Hz GPS and strong motion data". J. Geod., vol. 95, pp. 121, 2021. DOI: https://doi.org/10.1007/s00190-021-01570-0

[23] Danciu, L., "Development of a system to assess the earthquake damage potential for buildings: Intensiometer" University of Patras, 2006. DOI: 10.12681/eadd/26457.

[24] Mori, F., Mendicelli, A., Falcone, G., Acunzo, G., Spacagna, R. L., Naso, G., and Moscatelli, M. "Ground motion prediction maps using seismic-microzonation data and machine learning", Nat. Hazards Earth Syst. Sci., vol 22, 947–966, 2022. DOI: https://doi.org/10.5194/nhess-22-947-2022.

[25] Elenas, A., "Seismic-Parameter-Based Statistical Procedures for the Approximate Assessment of Structural Damage", Mathematical Problems in Engineering, vol 2014, 1024-1045, 2014. DOI: https://doi.org/10.1155/2014/916820

[26] Lin, J., Smerzini, C. "Variability of physics-based simulated ground motions in Thessaloniki urban area andits implications for seismic risk assessment", Front. Earth Sci. 10:951781, 2022. DOI: 10.3389/feart.2022.951781